Reduction of Power Fluctuation in Wind Turbine Using Variable Frequency Transformer and Optimized PID Controller

Chellaswamy C[1,*], Muthammal R[2] Pragadeeshkumar N[3] and Ramesh R[4]

[1]Department of Electronics and Communication Engineering, Rajalakshmi Institute of Technology
Chennai, India

[2]Department of Electronics and Communication Engineering, Sri Ram Engineering College
Chennai, India

[3]Department of Electronics and Communication Engineering, Rajalakshmi Institute of Technology
Chennai, India

[4]Department of Electronics and Communication Engineering, Saveetha Engineering College
Chennai, India

[*]*Corresponding author's email: chella_info [AT] yahoo.co.in*

ABSTRACT—*This manuscript describes the possibility of permanent magnet synchronous generator (PMSG) based wind energy generation using variable frequency transformer (VFT)with an optimized particle swarm optimization based PID (PSO-PID) controller for reducing power fluctuations. VFT is a recent power transmission technique used to eliminate the power electronics needed in the conventional wind energy conversion system. To analyze the performance of the proposed method the MATLAB-Simulink model has been developed and tested under various loading condition. The efficiency of the proposed method has been verified by comparing the total harmonic distortion (THD) of the output voltage, current, and efficiency of the proposed method with the conventional method. The simulation results indicate that the proposed PSO-PID method does not produce harmonics and easy to implement. The cost analysis has been carried out and it shows that the proposed method is cheaper than the conventional method of generating wind power.*

Keywords— permanent magnet synchronous generator, variable frequency transformer, particle swarm optimization, PID controller, wind turbine

1. INTRODUCTION

Due to the anxiety of the atmosphere, the power generation based on renewable energy (RE) is necessary. The utilization of solar, hydro, and wind power generation has been increased. Generally, a RE based wind generation needs a power grid for reliable power supply. On the other hand, the power generation in remote location can easily serve the local load as a result reduction of transmission loss, eliminating grid connection, and save transmission cost [1]. To develop a wind power generation and use the wind properly, a fixed and a variable speed wind energy conversion systems are used. The induction generators are familiarly used in fixed speed wind turbine because of its ruggedness, less maintenance, and simple design [2]. The fixed speed wind turbine require high starting current and stipulate to reactive power [3]. Variable speed wind turbines (VSWT) has different advantages such as maximum power point operation, higher energy capture, improved power quality, and high efficiency. Hence, the VSWT take over the wind power generation and sophisticated electronic converters are used to connect them into the grid. In addition, the electronic converters produce harmonic distortion as a result the quality of power will be decreased and by introducing suitable compensation technique the harmonic can be reduced [4].

The PMSG is the familiarly used wind power generator in small scale renewable power plants. The climatical condition affects the performance of wind power generation and multi-pole low speed PMSG are used to overcome these difficulties [5]. The gear box which is connected with the generator creates many technical problems such as produce noise, increase the total weight of the plant, increase the power loss, and need regular maintenance. The low speed PMSG can solve these problems by direct drive [6]. The VFT is a wound-rotor induction machine (WIM) and do the bidirectional power transmission ie. transfer active from one power network to the other. VFT has a WIM which is driven by a dc drive motor. The mechanical torque applied to the WIM rotor shaft decides the active power transfer from

VFT [7]. The stator and rotor windings of the WIM of the VFT are connected to the grid and to the ac bus respectively. Both the windings are connected through a compensation capacitor bank. The stability analysis of VFT has not been carried out perfectly and most of the estimated results are in time domain [8]. The grid connected wind turbine with VFT has been studied in [9]. A proportional integral differential (PID) controller is used to reduce the power fluctuations. An alternative configuration is designed for VFT and the performance has been studied in [10].

Various studies related to the steady state analysis of VFT has been carried out in the literatures [11,12]. Ekanayake et al. proposed a simplified model of doubly fed induction generator and compared the performance with fifth and third order model. Various faulted circumstances of PMSG has been considered and analyzed in [13]. In this paper, we have proposed an alternate method to design a controller using particle swarm optimization (PSO) to reduce the power fluctuations based on KO et al. [14]. A sixth order transfer function has been taken from [15, 16] for analysis. Comparison has been made with the existing solution related to power system with grid disturbance. This paper has been established as follows. The proposed system with VFT and the optimized PID controller is described in section 1. However, in section-3, the PSO algorithm has been described. The simulation results has been described in section 4. Finally, the conclusion is explained in section 5.

2. PROPOSED SYSTEM

The VFT provides a flexible link between the PMSG and the grid. In the proposed system, the wind turbine is directly connected to the PMSG and the output of the PMSG is fed to the VFT. The proposed system does not require gear box and is shown in Fig. 1. The rotor and the stator winding of doubly-fed wound rotor induction machine (DWRIM) is connected with the stator winding of PMSG and to the power grid respectively. To control the power flow of PMSG a DC drive motor has been connected to the rotor of DWRIM. On the other hand, in the conventional wind power generation system, the gear box is connected between turbine and PMSG. Moreover, a power electronic conversion system (ac-dc and dc-ac) is incorporated in the conventional power generation system and it will produce harmonic distortion at the output.

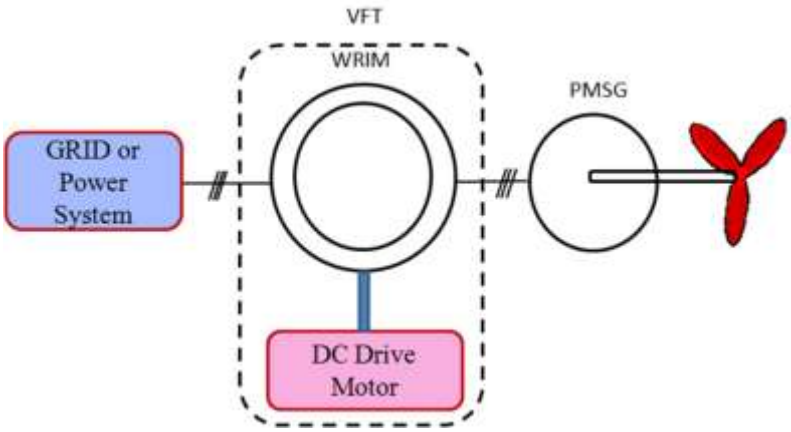

Figure 1: Proposed system connected with PMSG.

2.1 Model of VFT

The VFT is directly coupled with a dc drive motor (DCDM) is shown in the Fig. 1. The DCDM is a dc motor which generates mechanical torque required to drive the shaft of the wound rotor induction machine (IM) of the VFT and the equivalent circuit of DCDM of VFT is shown in Fig. 2. The voltage current (p.u) equation of DCDM can be expressed based on [17] as:

$$\left(\frac{L_{mt}}{\omega}\right) d(I_m) = V_m - e_a - R_m I_m \tag{1}$$

Where L_{mt} is the equivalent inductance of armature (p.u), d represents the differential operator with respect to time, ω is the rotational speed, I_m and V_m are the current and voltage of DCDM (p.u) respectively. R_m and e_a are the equivalent resistance and counter electromotive force of the armature respectively. Here we are assuming that the field current of DCDM is constant. The rotational speed and the generating torque of the DCDM can be controlled by V_m. The controller block diagram of DCDM is shown in Fig. 3. The entailed torque produced by the DCDM can be easily obtained from the controlling value of V_m. The controller of DCDM can be can expressed (p.u) as:

$$(T_L) d(\Delta V_m) = K_1 \left(P_{ref} - P_{oa}\right) - \Delta V_m \tag{2}$$

Where T_L and K_1 represents the time constant and gain of the control loop, ΔV_m is the deviation in active power, P_{oa} is the output active power of the VFT and P_r is the output active power of the PMSG.

The torque T_q has been applied to the rotor of DWRIM by the dc drive motor and the position of rotor can be adjusted relative to the stator. The stator winding of the DWRIM is energized by the grid voltage and the phase angle V_{gd} and ϕ_{gd} respectively. The torque applied and the power flow through VFT is proportional to each other [18]. In this study, the real power transfer has been discussed. The power flow through VFT can be expressed based on [19] as :

$$P_{VFT} = P_{peak} \times sin\theta_{tot} \tag{3}$$

where P_{VFT} and P_{peak} are the power flow through VFT and peak flow possible through VFT when Θ_{tot} is 90°. The peak power is expressed as:

$$P_{peak} = \frac{V_{gd} \times V_{pg}}{X_{mut}} \tag{4}$$

where V_{gd} and V_{pg} denotes the voltage magnitude of grid and PMSG respectively. X_{mut} represents the total reactance between the grid to PMSG. The total phase angle can be written as $\Theta_{tot} = \Theta_{gd}-(\Theta_{pg} - \Theta_{ms})$. where Θ_{ms} is the phase angle of rotor of PMSG due to Θ_{pg} according to the stator due to Θ_{gd}. Now the equation (2) cab be written as:

$$P_{VFT} = \frac{V_{gd} \times V_{pg}}{X_{mut}} \times sin\left[\theta_{gd} - \left(\theta_{pg} + \theta_{ms}\right)\right] \tag{5}$$

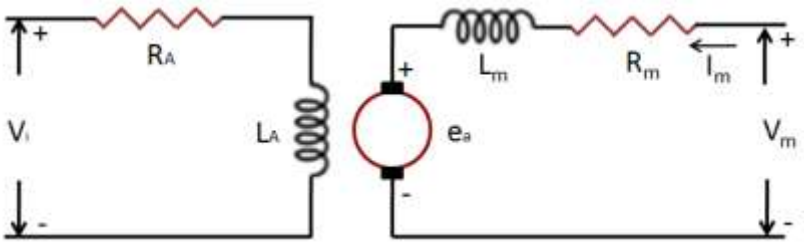

Figure 2: Equivalent circuit of the dc drive motor with the VFT.

2.2 PID Controller for DCDM

The DCDM of VFT incorporating the PID controller is shown in Fig. 3. The PID controller contain the active power deviation (δ_p) which is the difference between the reference power (P_{ref}) of the ac bus and the active power (P_a). The small value of δ_p is used to control the DCDM of VFT as a result improvement in power flow and stability can be achieved. The feedback signal (P_f) is used to enhance the poorly damped modes [20, 21]. The input (X) and output (Y) vector can be expressed as:

$$X = P_a \tag{6}$$

$$Y = \delta_p \tag{7}$$

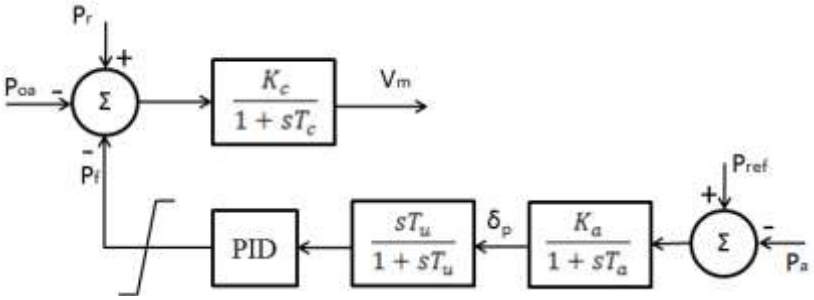

Figure 3: Block diagram of the PID controller.

The transfer function H(S) of the VFT controller can be expressed based on (6) and (7) as:

$$H(S) = \frac{X(S)}{Y(S)} = \frac{P_f(S)}{\delta_p(S)} \tag{8}$$

$$= \frac{sT_u}{1+sT_u}\left(K_P + \frac{KI}{s} + sK_D\right) \tag{9}$$

where T_u is the time constant of unsuccessful term and K_P, K_I, and K_D are the gain values of the PID controller.

3. PARTICLE SWARM OPTIMIZATION

The particle swarm optimization an innovative progression computational algorithm used to solve the nonlinear problems. This process is established on the congregate activities (ex: detect food using flocking) of birds.

3.1 PSO Algorithmic rule

Particle swarm optimization (PSO) is a population based stochastic optimization technique which has the behaviors of bird flocking developed by Dr. Eberhart and Dr. Kennedy in 1995. PSO is initialized with a group of random particles (solutions) and then searches for optima by updating generations. Through every iteration, each particle has been updated and store the estimates the "best" solution called local best solution. The particle swarm optimizer track the another best value called global best value [22].

The D-dimensional search space contains k^{th} particles and it can be symbolized as $X_k=(X_{k1}, X_{k2}, X_{k3}, ..., X_{kd})$ and the best position of the particle can be described as $Mbest=(Mbest_{k,1}\ Mbest_{k,2}\ Mbest_{k,3},..., Mbest_{k,d})$. The best particle amongst the set is Gbest and the velocity of the k^{th} particle is denoted by $V_k=(V_{k,1}\ V_{k,2}\ V_{k,3}, ..., V_{k,d})$. The distance between Mbest to the Gbest can be updated based on [23].

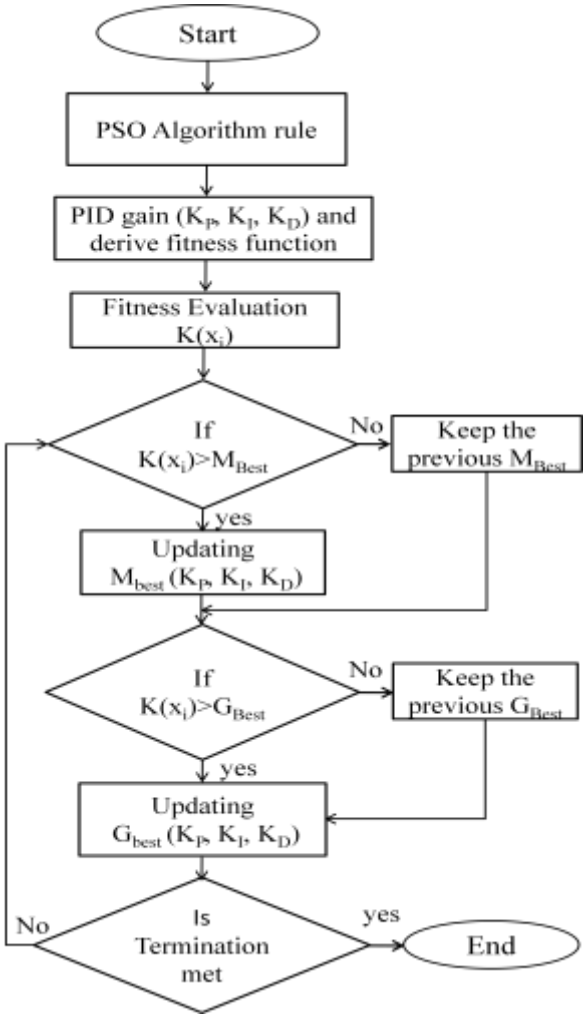

Figure 4: Flow diagram of the PSO based PID controller

3.2 PID design approach

Here, 3-D search space for the PSO structure is assigned to the PID parameters K_P, K_I, and K_D. The fitness function is used to alter the time domain values. Further, the values of numerals can be adjusted during the computation. To optimize all the parameters of PID and getting best results, all the parameters are present in all 3-dimensions. Every point in the search space has the value of the arguments [K_P, K_I, K_D]. The fitness function determines the position and the precise value of the PID parameters. The fitness function consist of other important features such as rise time, peak overshoot, steady state errors, and settling time. The fitness function can be expressed as:

$$F_{fit} = 1 - e^{-\delta}(M_{peak} + E_{ss}) + e^{-\delta}(T_{ST} - T_{RT}) \quad (10)$$

where F_{fit}, δ, Mp, E_{ss}, T_{ST} and T_{RT} are represents the fitness function, scaling factor, peak overshoot, steady state error, settling time, and rise time respectively. To determine the best value from the fitness function we have developed a MATLAB function fitness(K_P, K_I, K_D) and PSO based gain has been estimates based on [24, 25]. The best fitness function value, fbest=0.1853, and after several iterations the gain parameters K_P, K_I, K_D values 38.821, 6.935, and 0.037 has been obtained. The flow diagram of the proposed PSO-PID controller for the proposed system is shown in Fig. 4. The following steps has been involved in the PSO-PID controller.

1. PSO description and the rules.
2. PSO approach to design the PID controller.
3. The PSO based controller gain K_P, K_I, K_D and define the fitness function.
4. The sixth order transfer function has been taken [24] to implement the fitness function.
5. Update M_{best} and G_{best} values.
6. For the best fitness value of the proposed system, the PSO-PID gain K_P, K_I, K_D has been described.

4. SIMULATION RESULTS

In this paper, the VFT is connected with the PMSG which has a doubly fed three phase, 420 V, 50 Hz, 5.5 kW. The three phase resistive load (420 V, 50 Hz) is connected to the rotor winding of DWRIM. The simulation is carries out using MATLAB-Simulink 2016, Intel core i5, 2.4 GHz with 16GB RAM computer. A model has been developed for the proposed system and is shown in Fig. 5. Various parameters such as stator voltage (Vs), stator frequency (f_s), power output (P_o), mechanical power supplied by the DCDM (P_{MP}), the slip of VFT (S_{VFT}), the load voltage and power, threshold of load voltage and power, and the efficiency has been studied.

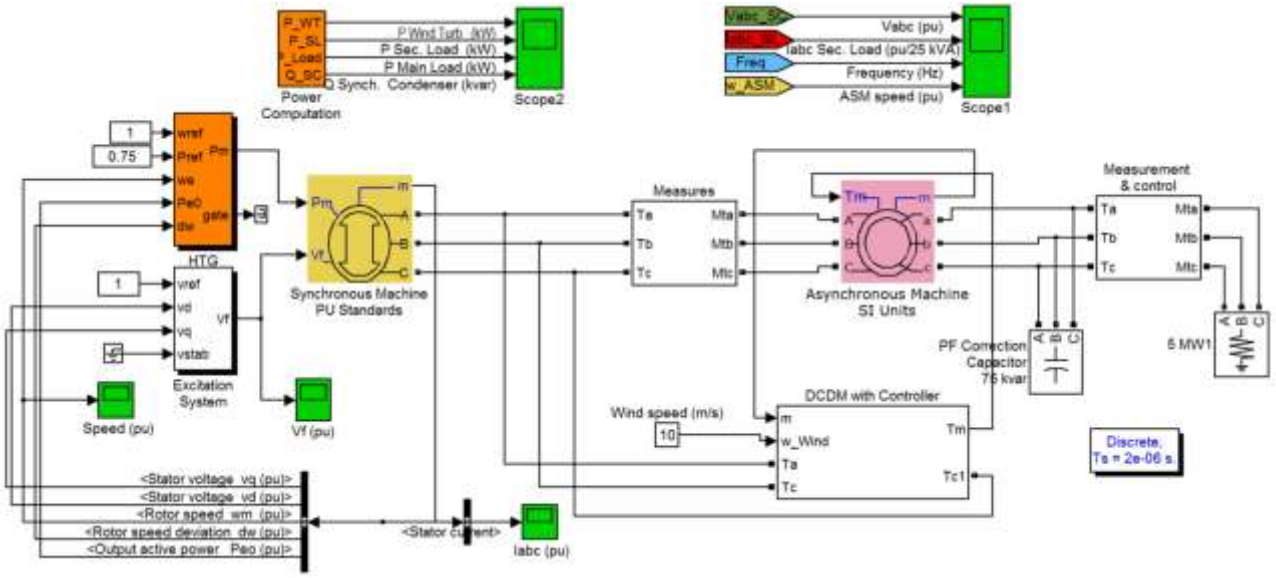

Figure 5: Simulation model for the proposed system

The speed of PMSG is varied and the other parameters such as the load frequency and voltage are kept constant. In order to provide the required reactive power to the stator of DWRIM a capacitor bank is connected between the stator winding of DWRIM. To study the performance of the proposed system, different loads such as 1 kW and 4 kW has been taken for various speed of SG. The speed control of DWRIM depends on the mechanical power of DCDM. To maintain constant load frequency the slip of VFT should be controlled because the load frequency depends on the slip of VFT. Various parameters obtained of different speeds of PMSG under two loading conditions is shown in Table 1. Table 1 indicates that the voltage at the stator terminals of PMSG at rated speed is almost equal to the rated voltage of 400 V and frequency of 50 Hz. The output voltage, power, and frequency of PMSG depends on the speed of PMSG. From Table 1 one can easily understand that the voltage, power, and frequency increased from 396 V to 397 V, the power from 986 W to 995 W and the frequency from 42.5 Hz to 44.6 Hz when the speed is increased from 1100 to 1200 rpm under 1 kW load. The torque applied by the DCDM depends on the speed of DWRIM and it is equal to the speed of PMSG is subtracted to the synchronous speed of the DWRIM. The output frequency is 50 Hz in this speed of DWRIM. If the speed of PMSG is decreased then the magnitude of output voltage and power will be reduced from its rated value. Further, the variation in THD value is 0.01% for the load current and voltage and it is negligible. The cost analysis of the

proposed system has been studied and compared with the conventional system is shown in Table. 2. The data required to estimate the cost analysis of both the proposed and conventional system has been taken and performed based on [26].

Table 1: Different parameters of PMSG and DWRIM for various speeds under two loading condition

SG speed (rpm)	V_s (V)	f_s (Hz)	P_o(W)	P_{MP} (W)	S_{VFT}	V_L (V)	P_L (W)	% THD of I_L	% THD of V_L	% η
1 kW load										
100	38.73	15.64	78.94	793.91	0.24	364.51	801.80	0.01	0.01	91.86
200	50.46	18.24	122.65	759.37	0.29	369.84	810.22	0.01	0.01	91.86
300	76.12	21.03	195.74	728.74	0.35	374.93	849.23	0.01	0.01	91.86
400	102.73	24.27	268.84	698.53	0.4	381.64	888.63	0.01	0.01	91.86
500	127.38	27.52	343.63	662.73	0.45	356.73	924.44	0.01	0.01	91.86
600	155.43	30.28	418.26	613.84	0.51	388.93	948.43	0.01	0.01	91.86
700	181.85	33.02	492.63	550.42	0.57	391.52	958.16	0.01	0.01	91.86
800	107.94	35.52	564.73	484.97	0.61	392.32	964.25	0.01	0.01	91.86
900	234.73	38.25	639.61	418.53	0.66	394.26	972.01	0.01	0.01	91.86
1000	261.94	41.01	717.14	350.96	0.71	395.49	980.94	0.01	0.01	91.84
1100	288.47	42.49	792.38	281.52	0.77	396.16	986.27	0.01	0.01	91.84
1200	314.63	44.59	871.83	212.74	0.83	397.52	995.96	0.01	0.01	91.83
4 kW load										
400	162.47	24.27	973.15	2546.57	0.267	360.03	3208.37	0.01	0.01	91.154
500	183.46	27.52	1253.69	2326.85	0.333	363.95	3263.87	0.01	0.01	91.156
600	204.63	30.28	1586.36	2186.46	0.400	367.46	3439.15	0.01	0.01	91.156
700	225.70	33.02	1895.57	1924.74	0.467	371.04	3482.44	0.01	0.01	91.156
800	246.78	35.52	2121.46	1763.65	0.533	375.75	3541.36	0.01	0.01	91.152
900	267.75	38.25	2440.35	1547.64	0.600	380.53	3635.13	0.01	0.01	91.152
1000	288.95	41.01	2761.43	1327.74	0.667	385.35	3727.19	0.01	0.01	91.148
1100	309.37	42.49	3082.67	1074.47	0.733	388.46	3789.15	0.01	0.01	91.148
1200	330.45	44.59	3410.56	824.75	0.800	391.73	3860.40	0.01	0.01	91.148
1300	351.74	46.21	3736.75	564.38	0.867	394.97	3920.35	0.01	0.01	91.147
1400	372.48	48.58	4063.57	274.64	0.933	397.89	3954.10	0.01	0.01	91.146

Table 2: Comparison of cost analysis between the proposed system and the conventional system.

Materials/Devices	Conventional System	Proposed System		
		PMSG	DWRIM	DCDM
Iron	32.5	32.5	4.15	1.42
Copper	12.78	12.78	1.32	0.48
Total (kg)	45.28	45.28	5.47	1.90
SG active material cost	289	289		
construction cost of SG	164	167		
DWRIM active material cost	-	32		
DCDM active material cost	-	11		
construction cost of DCDM and DWRIM	-	42		
Converter cost	124	-		
Total cost ($)	577	541		

Table 2 indicates that the cost required for the proposed system is less than that of the conventional system. The terminal output voltage and current of PMSG using conventional and the proposed PSO-PID method is shown in Fig.6 and 7 respectively. From Fig. 6 and 7 one can easily understand that the terminal voltage and current of the proposed PSO-PID had been improved compared to conventional controller. The steady state analysis of the proposed system including VFT and PSO-PID controller under various wind speed has been studied. Here, the cut-in wind speed of 5 m/s and the cut-out wind speed of 22 m/s has been taken to estimate the deviations present in the steady state condition of the proposed system with PSO-PID controller. The rated speed of 15 m/s has been taken and different parameters has been studied under steady condition and is shown in Fig. 8.

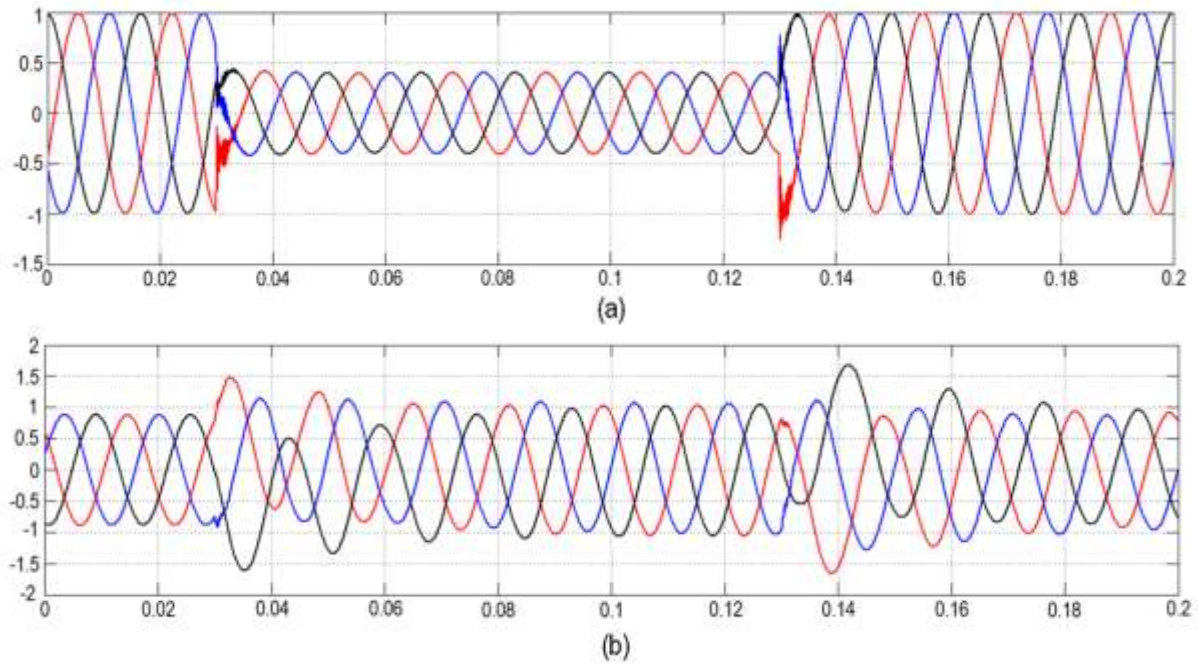

Figure 6: Terminal output of PMSG using conventional method (a) voltage (b) current

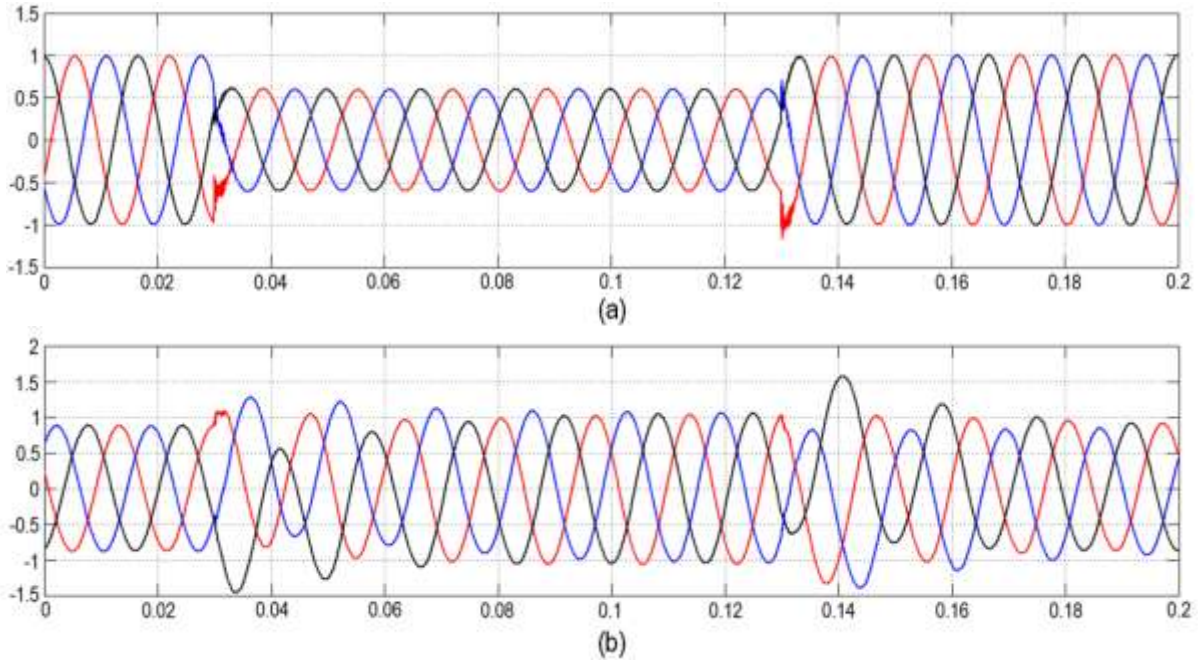

Figure 7: Terminal output of PMSG using PSO-PID method (a) voltage (b) current

Fig. 8 (a) shows that the performance of pitch angle of wind turbine. The pitch angle of the turbine maintain almost zero up to certain value and slowly increase from 0 to certain limit to maximize the output current and active power of the wind turbine. The output reactive power is around 0 p.u, hence the output power factor is near to unity. When the wind turbine speed varies from cut-in speed to rated speed then the rotor speed will vary from sub-synchronous speed to

super synchronous speed and the performance of DCDM of the VFT is shown in Fig. 8 (b). The voltage of stator winding (V_{SW}) and the voltage of rotor winding (I_{SW}) have been maintained at 1 p.u for all the wind speed scenario. The stator winding reactive power (Q_{SW}) of IM of the VFT is kept constant. The active power and the stator winding current rapidly increases at start and maintain constant (1 pu) V at 14 m/s. The value of V_m , I_m and Tv are shown in Fig. 8 (c). On the other hand, the rotor speed of IM ad DCDM are rapidly increases from the start and maintain constant at 14 m/s very quickly and is shown in Fig. 8 (d).

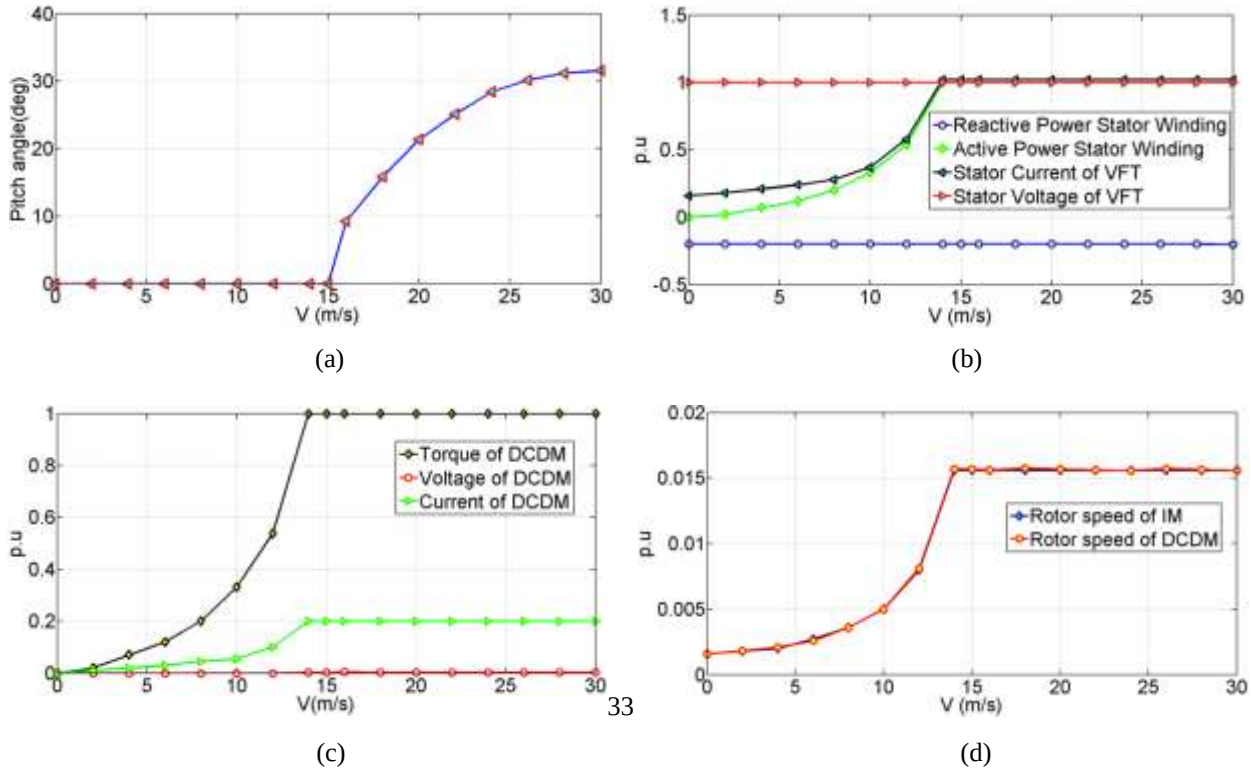

Figure 8: Steady state condition of the proposed system under different wind speed (a) wind turbine pitch angle (b) VFT (c) DCDM of VFT (d) rotor speed of IM and DCDM of the VFT

The performance of PID controller used in the VFT has been studied under a burst wind disturbance. Here the output performance has been carried out by including VFT, VFT with the PID controller, and VFT with the PSO-PID controller is shown in Fig. 9. For simulation, the initial wind speed is around 11 m/s when 0<t<6s, the wind speed rapidly arrive at 13.7 m/s when 6<t<13, the wind speed is reduced to 11.8 m/s when 13<t<16s, and the wind speed is further reduced to 11.2 m/s and maintain almost in the same state has been taken. The dynamic response of the proposed system is shown in Fig. 9. Fig 9 (a) and (b) illustrates that the active and reactive power of the VFT with PID and PSO-PID controller. The rotor speed of the proposed system play a significant effect on active power of the turbine. It is clearly observed from Fig. 9. (c) and (d) that even noticeable oscillation is present in the active and reactive power the proposed PSO-PID controller efficiently reduces the variation.

Table 3: Comparison of peak time, rise time, settling time, and peak overshoot between the conventional and proposed PSO-PID controller.

Controller	Peak time	Rise time	Settling time	Peak overshoot
Conventional PID	0.1569	0.0173	0.5864	16.0532
PSO-PID	0	0	0.4183	0.

The performance comparison of peak time, rise time, settling time, and peak overshoot between the conventional and proposed PSO-PID controller is shown in Table 3. From Table 3 one can easily understand that the PSO-PID controller reduces the steady state error to zero. The response of the proposed PSO-PID does not have much under-damped signal and the other parameter such as peak time, rise time, and peak overshoot has been reduced to zero. Hence, the PSO-PID eliminate reactive power variation in the PMSG.

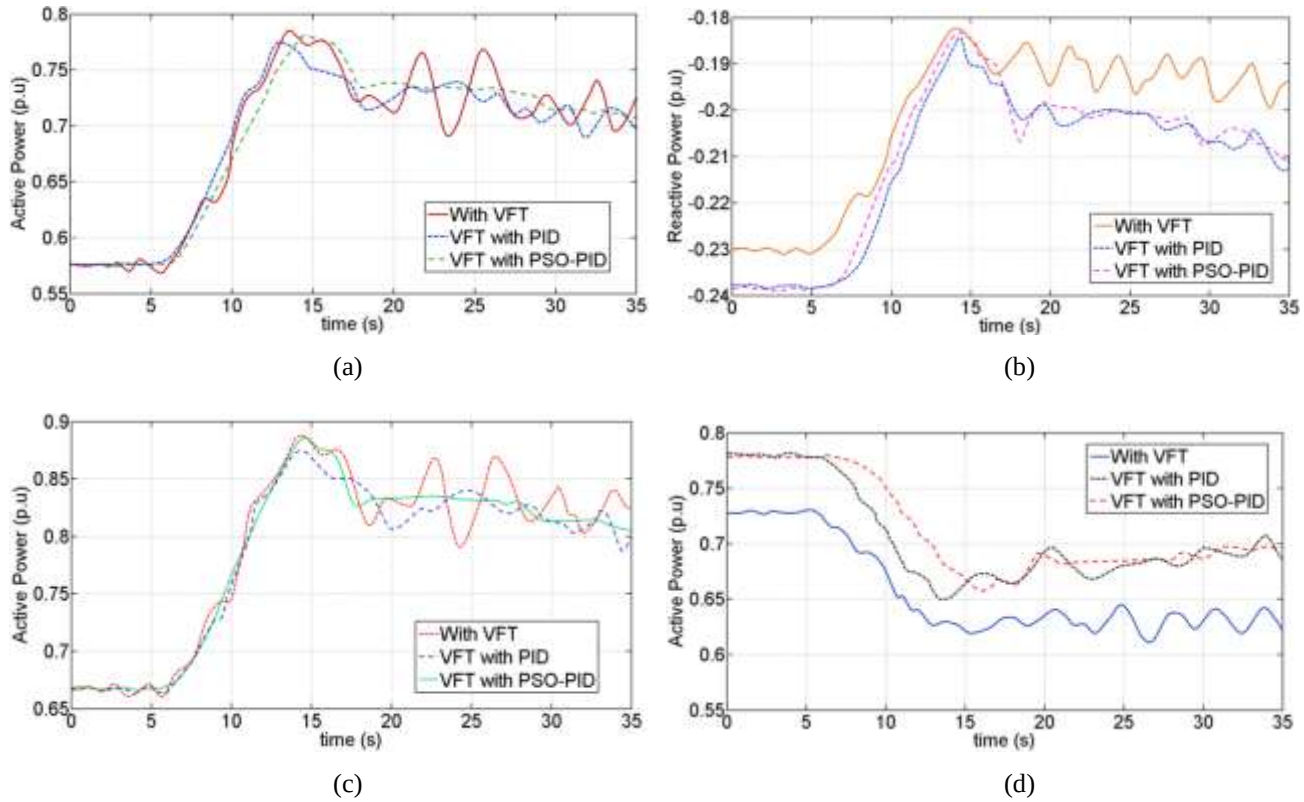

Figure 9: Dynamic response of the proposed system under a burst wind disturbance (a,b) active and reactive power of VFT (c,d) active and reactive power of grid.

5. CONCLUSION

This paper has presented a VFT based grid connected wind power generation system using PSO-PID controller. The simulation has been carried out using MATLAB software. It shows that the VFT performs reduction of power fluctuation and active power control. The efficacy of the VFT with the PID and PSO-PID controller has been studied under different wind speed condition. From the steady state results, it can be concluded that by adjusting the output torque of the DCDM of the VFT the generated active power can be easily transferred to the grid line. The inherent variations present in the generated output of simulated response can be reduced efficiently by the proposed system with PSO-PID controller.

6. REFERENCES

[1] L.A. de S. Ribeiro, O.R. Saavedra, S.L. Lima, J.G. de Matos, G. Bonan, "Making isolated renewable energy systems more reliable", Renew. Energy, (Elsevier) vol. 45, pp. 221-231, 2012.
[2] F.I. Bakhsh, M.M. Shees, M.S.J. Asghar, "Performance of wound rotor induction generators with the combination of input voltage and slip power control", Russ. Electr. Eng., vol. 85, no. 6, pp. 403-417, 2014.
[3] Bhadra SN, Kastha D, Banerjee S, Wind electrical systems, Oxford Press, 2006.
[4] Bhende CN, Mishra S, Malla SG, "Permanent magnet synchronous generator based standalone wind energy supply system", IEEE Trans Sust Energy, vol. 2, no. 4, pp. 361-73, 2011.
[5] C. Mi, M. Filippa, J. Shen, N. Natarajan, "Modeling and control of a variable-speed constant-frequency synchronous generator with brushless exciter", IEEE Trans Ind Appl, vol. 40, no. 2, pp. 565-73, 2004.
[6] AJG Westlake, JR Bumby, E. Spooner, "Damping the power-angle oscillations of a permanent-magnet synchronous generator with particular reference to wind turbine applications", IEE Proc Electr Power Appl, vol. 143, no. 3, pp. 269-80, 1996.
[7] E.R. Pratico, C. Wegner, E.V. Larsen, R.J. Piwko, D.R. Wallace, D. Kidd, "VFT operational overview -The laredo project," in Proc. of the IEEE Power Engineering Society General Meeting, USA, 2007.
[8] A. Merkhouf, P. Doyon, S. Uphadayay, "Variable frequency transformer—Concept and electromagnetic design evaluation", IEEE Trans. Energy Conversion, vol. 23, no. 4, pp. 989-996, 2008.
[9] L. Wang and L. Y. Chen, "Reduction of power fluctuations of a large scale grid-connected offshore wind farm using a variable frequency transformer", IEEE Trans. Sustain. Energy, vol. 2, no. 3, pp. 226-234, 2011.

[10] A.S. Abdel-Khalik, A. Elserougi, S. Ahmed, A. Massoud, "Brushless doubly fed induction machine as a variable frequency transformer", in Proc. 6th IET Int. Conf. Power Electron., Mach. Drives, pp. 1–6, 2012.
[11] L. Contreras-Aguilar, N. Garcia, "Fast convergence to the steady state operating point of a VFT park using the limit cycle method and a reduced order model", In Proc. IEEE Power Eng. Soc. Gen. Meeting, Calgary, Canada, pp. 1–5, 2009.
[12] E. T. Raslan, A. S. Abdel-Khalik, M. Abdulla, M. Z. Mustafa, "Performance of VFT when connecting two power grids operating under different frequencies", in Proc. 5th IET Int. Conf. Power Electron., Mach. Drives, pp. 1–6, 2010.
[13] J.B. Ekanayake L. Holdsworth, N. Jenkins, "Comparison of 5th order and 3rd order machine models for doubly fed induction generator (DFIG) wind turbines", Electric Power Systems Research 67, pp. 207-215, 2003.
[14] Hee-Sang KO, Gi-Gab Yoon, Nam-Ho Kyung, Won-Pyo Hong, "Modeling and control of DFIG-based variable speed wind-turbine", Electric power system Research, vol. 78, pp. 1841-1849, 2008.
[15] N.S. Nise, Control Systems Engineering, John Wiley & Sons, Hoboken, USA, 2008.
[16] T. Ackermann, Wind Power in Power Systems, John Wiley & Sons, Hoboken, USA, 2008.
[17] S. Heier, Grid Integration of Wind Energy Conversion Systems. New York: John Wiley & Sons, 1998.
[18] Merkhouf A, Doyon P, Upadhyay S. "Variable frequency transformer – concept and electromagnetic design evaluation", IEEE Trans Energy Conversion, vol. 23, no. 4, pp. 989–96, 2008.
[19] R. J. Piwko, E. V. Larsen, C. A. Wegner, "Variable frequency transformer-a new alternative for asynchronous power transfer", in Proc. IEEE Power Eng. Soc. Conf. Expo., Durban, pp. 393–398, 2005.
[20] M. N. Anwar, S. Pan, "A new PID load frequency controller design method in frequency domain through direct synthesis approach", Electrical Power and Energy Systems, vol. 67, pp. 560-569, 2015.
[21] Mary A.G Ezhil, Joseph Jawhar, Chellaswamy C, "Optimized PIDF controller for enhancing stability in power system with UPFC and Redox flow batteries", International Journal of Applied Engineering Research, Vol. 11, no. 8, pp. 14902-15913. 2016.
[22] Y. Valle, G.K. Venayagamoorthy, S. Mohagheghi, J.C. Hernandez, R.G. Harley, "Particle swarm optimization: Basic concepts, variants an applications in power systems", IEEE Transactions on Evol. Comput., vol. 12, pp. 171-195, 2008.
[23] Russell C. Eberhart, Yuhui Shi, "Particle Swarm Optimization: Developments, Applications, and Resources", Evolutionary Computation, Proceedings of the IEEE Congress, pp. 27-30, 2001.
[24] Om Prakash Bharti, R. K. Saket, S. K. Nagar, "Controller Design For DFIG Driven By Variable Speed Wind Turbine Using Static Output Feedback Technique", Engineering, Technology & Applied Science Research, vol. 6, No. 4, pp-1056-1061, 2016.
[25] C. Chellaswamy, R. Ramesh, C.Y. Visveswar Rau, "A supervisory control of a fuel free electric vehicle for green environment", IEEE International Conference on Emerging Trends in Electrical Engineering and Energy Management, pp. 387-393, 2012.
[26] H. Polinder, F.F.A. van der Pijl, G.J. de Vilder, P. Tavner, "Comparison of direct-drive and geared generator concepts for wind turbines", IEEE Trans. Energy Convers., vol. 21, no. 3, pp. 725-733, 2006.